Amorphous LiSiON Thin Film Electrolyte for All-solid-state Thin Film Lithium Battery

XIA Qiuying, SUN Shuo, ZAN Feng, XU Jing, XIA Hui

(School of Materials Science and Engineering, Nanjing University of Science and Technology, Nanjing 210094, China)

Abstract: All-solid-state thin film lithium battery (TFLB) is regarded as the ideal power source for microelectronic devices. However, the relatively low ionic conductivity of amorphous solid-state electrolyte limits the improvement of electrochemical performance for TFLB. In this work, amorphous lithium silicon oxynitride (LiSiON) thin films are prepared by magnetron sputtering as solid-state electrolyte for TFLB. With optimized deposition condition, the LiSiON thin film exhibits a high ionic conductivity of 6.3×10^{-6} S·cm^{-1} at room temperature and a wide voltage window over 5 V, making it a suitable thin film electrolyte for TFLB. A MoO$_3$/LiSiON/Li TFLB is constructed based on the LiSiON thin film electrolyte with large specific capacity (282 mAh·g^{-1} at 50 mA·g^{-1}), good rate capability (50 mAh·g^{-1} at 800 mA·g^{-1}), and acceptable cycle life (78.1% capacity retention after 200 cycles), demonstrating the feasibility of this electrolyte for practical applications.

Key words: LiSiON; thin film electrolyte; all-solid-state lithium battery; thin film battery

The rapid development of microelectronics industry, such as micro-electromechanical systems (MEMS), micro sensors, intelligent cards, and implantable micro medical devices, leads to increasing demands for integrated micro-sized energy storage[1-2]. Among the available battery technologies, all-solid-state thin film lithium battery (TFLB) is considered as the ideal power source for microelectronic devices due to their high safety, small size, power-on-chip design, long cycle life, and low self-discharge rate. As one of the key components in TFLB, solid-state thin film electrolyte plays a vital role in determining the properties of TFLB[3]. Therefore, developing high-performance solid-state thin film electrolyte is always an important goal for the development of TFLB. At present, the most widely used electrolyte in TFLB is amorphous lithium phosphorus oxynitride (LiPON), which has moderate ionic conductivity (2×10^{-6} S·cm^{-1}), low electronic conductivity (~10^{-14} S·cm^{-1}), wide voltage window (~5.5 V), and good contact stability with lithium[4-5]. However, its ionic conductivity is relatively low, which impedes the future development of high power TFLB for the upcoming era of the Internet of Things (IoT)[6]. Thus, it is urgent to develop new thin film electrolytes with increased ionic conductivity, as well as large voltage window and good contact stability with lithium for next-generation TFLB.

Among various inorganic solid-state electrolyte materials, the Li$_2$O-SiO$_2$ solid solution system and their deuterogenic phases were identified as potential thin film electrolytes due to their fast three-dimensional lithium conduction channels[7]. For example, Chen, *et al*.[8] reported that Al substituted Li$_{4.4}$Al$_{0.4}$Si$_{0.6}$O$_4$-0.3Li$_2$O solid electrolyte has a high ionic conductivity of 5.4×10^{-3} S·cm^{-1} at 200 ℃. Adnan, *et al*.[9] found that Li$_4$Sn$_{0.02}$Si$_{0.98}$O$_4$ compound possesses a maximum conductivity value of 3.07×10^{-5} S·cm^{-1} at ambient temperature. However, previous works on Li$_2$O-SiO$_2$ electrolyte systems mostly focused on powder materials with high crystallinity, while very limited work was reported on their amorphous thin film counterparts for TFLB. Since TFLB is typically constructed by depositing thin films of cathode, electrolyte and anode layer by layer, the electrolyte film is required to be prepared at relatively low temperature to avoid the unfavorable interactions between the cathode and electrolyte, which result in crack and short circuit of the TFLB[1-2]. Thus, developing Li$_2$O-SiO$_2$ electrolyte with amorphous feature prepared at low temperature is important for TFLB.

Although recent work[6] shows that a high lithium ionic conductivity of 2.06×10^{-5} S·cm^{-1} can be obtained by amorphous Li-Si-P-O-N thin film, its contact stability with the electrodes and electrochemical stability in TFLB have yet to be investigated. Therefore, it is critically important to develop high-performance Li_2O-SiO_2 based thin film electrolyte and demonstrate its actual application in TFLB.

In this work, amorphous lithium silicon oxynitride (LiSiON) thin film was prepared by radio frequency (RF) magnetron sputtering at room temperature and investigated as solid-state electrolyte for TFLB. The sputtering power and the flow of N_2/Ar working gas were optimized to obtain the best deposition condition for the LiSiON thin film. Moreover, to demonstrate the applicability of the optimized LiSiON electrolyte for TFLB, a MoO_3/LiSiON/Li full cell was constructed and its electrochemical performance was systematically investigated.

1　Experimental

1.1　Preparation of LiSiON thin films

LiSiON thin films were prepared by RF magnetron sputtering (Kurt J. Lesker) using a Li_2SiO_3 target (76.2 mm in diameter) at room temperature for 12 h. Before deposition, the pressure of the chamber was reduced to less than 1×10^{-5} Pa. The distance from target to substrate was 10 cm. The samples deposited under RF power of 80, 100, and 120 W at the flow of 90 sccm N_2 are marked as sample LiSiON-80N9, LiSiON-100N9, and LiSiON-120N9, respectively. And the samples deposited under RF power of 100 W at the flow of 90 sccm N_2 and 10 sccm Ar, 90 sccm N_2 and 50 sccm Ar, 50 sccm N_2 and 50 sccm Ar are marked as sample LiSiON-100N9A1, LiSiON-100N9A5, and LiSiON-100N5A5, respectively.

1.2　Preparation of MoO₃/LiSiON/Li TFLB

MoO_3 film was prepared by direct current (DC) reactive magnetron sputtering (Kurt J. Lesker) using a pure metal Mo target (76.2 mm in diameter) according to our previous report[10]. The distance from target to substrate was 10 cm, and DC sputtering power was 60 W. The deposition was performed at the substrate temperature of 100 ℃ for 4 h at the flow of 40 sccm Ar and 10 sccm O_2, followed by an *in-situ* annealing treatment at 450 ℃ for 1 h. LiSiON-100N9A1 was then deposited on the MoO_3 film as electrolyte. After that, a metallic lithium film of about 2 μm in thickness was deposited on the LiSiON film by vacuum thermal evaporation (Kurt J. Lesker). The final fabrication step involved the deposition of Cu current collector and the encapsulation process.

1.3　Material characterization

The crystal structures of the samples were characterized by X-ray diffraction (XRD, Bruker D8 Advance). The morphologies and microstructures of the samples were characterized by field emission scanning electron microscope (FESEM, FEI Quanta 250F) equipped with energy-dispersive X-ray spectroscopy (EDS). The elemental compositions of the samples were analyzed by inductively coupled plasma mass spectrometry (ICP-MS, Agilent 7700X). The chemical composition and bonding information of the samples were measured by X-ray photoelectron spectroscopy (XPS, Escalab 250XI, Thermo Scientific).

1.4　Electrochemical measurements

The ionic conductivity of the LiSiON thin film electrolyte was measured using a sandwiched structure of Pt/LiSiON/Pt. The electrochemical impedance spectroscopy (EIS) (from 1000 kHz to 0.1 Hz with potential amplitude of 5 mV) and cyclic voltammetry (CV) measurements of the samples were carried out on the Biologic VMP3 electrochemical workstation. Galvanostatic charge/discharge (GCD) measurement of the MoO_3/LiSiON/Li TFLB was carried out using a Neware BTS4000 battery system in an argon-filled glove box at room temperature. A Sartorius Analytical Balance (CPA225D, with resolution of 10 μg) was used to determine the electrode mass loading, and the mass loading of the MoO_3 film is about 0.4 mg·cm^{-2}.

2　Results and discussion

As shown in the optical image inserted in Fig. 1(a), a Li_2SiO_3 target was employed to prepare LiSiON thin film. The XRD result in Fig. 1(a) reveals that the target is composed of the major Li_2SiO_3 (JCPDS 83-1517) phase and minor SiO_2 phase. ICP-MS measurement indicates that the atomic ratio of Li∶Si is about 1.79∶1 in the target. Transparent amorphous thin film was obtained for the typical sample LiSiON-100N9A1 after sputtering the target (Fig. 1(b)). The thickness of the typical sample LiSiON-100N9A1 measured from the cross-section FESEM image in Fig. 1(c) is about 1.2 μm, indicating a growth rate of about 100 nm·h^{-1} under this condition. As shown in the top-view FESEM image in Fig. 1(d), the surface of the LiSiON thin film is very smooth and dense without cracks or pinholes, making it a suitable solid electrolyte for TFLB to avoid shortcut and safety problem.

XPS analysis was carried out to investigate the chemical composition and bonding information of the Li_2SiO_3
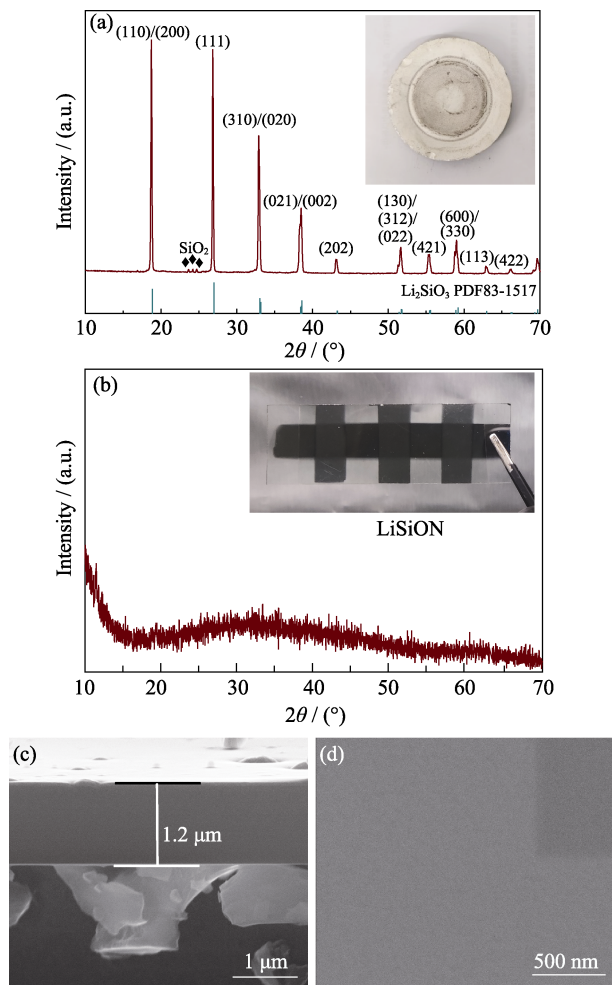
Fig. 1 (a) XRD pattern and optical image of the Li$_2$SiO$_3$ target; (b) XRD pattern and optical image of typical sample LiSiON-100N9A1; (c) Cross-section and (d) top-view FESEM images of the typical sample LiSiON-100N9A1

target and typical sample LiSiON-100N9A1. The XPS survey scan spectra in Fig. 2(a) reveal the presence of Li, Si, and O elements in the Li$_2$SiO$_3$ target and the introduction of N element in the LiSiON thin film. The atomic ratio of N : Si in LiSiON thin film is about 0.33 : 1 according to the XPS result. Combining with the corresponding atomic ratio (1.51 : 1) obtained by the ICP-MS measurement, the stoichiometry of the typical sample LiSiON-100N9A1 is determined to be Li$_{1.51}$SiO$_{2.26}$N$_{0.33}$. Compared with the single Si–Si (103.2 eV) peak in the Si2p core-level XPS spectrum of the Li$_2$SiO$_3$ target (Fig. 2(b)), additional Si–N (101.6 eV) peak can be observed from the LiSiON thin film, suggesting the occurrence of nitridation in LiSiON[11-12]. The O1s core-level XPS spectrum of Li$_2$SiO$_3$ target in Fig. 2(c) shows two bonding environments: 531.5 eV originated from SiO$_x$ and 528.8 eV assigned to Li$_2$O. After deposition, additional component emerged at 530.2 eV can be observed with LiSiON thin film, which can be assigned to nonbridging oxygen (O$_n$) in sili-

cate[13-14]. The N1s core-level XPS spectrum of LiSiON thin film in Fig. 2(d) can be deconvoluted into three peaks, including 398.2 eV for Si–N bonding, 396.4 eV for Li$_3$N, and 403.8 eV for nitrite species NO$_2^-$, further confirming the incorporation of N into the LiSiON network[14-16]. As schematically illustrated in Fig. 2(e), the incorporation of N into the LiSiON network can form more cross-linked structure, which is beneficial for fast lithium ion conduction[6,17].

To optimize the ionic conductivity and electrochemical stability of the LiSiON thin films, various LiSiON thin films deposited at different sputtering powers, and working gas flows were compared in terms of their ionic conductivities and voltage windows. The room-temperature Nyquist plots of the LiSiON thin films are depicted in Fig. 3(a), and the corresponding Pt/LiSiON/Pt sandwich structure and equivalent circuit are shown in Fig. 3(b). As observed, the Nyquist plots exhibit a single semicircle and dielectric capacitance tail, which is characteristic of thin-film conducting dielectric with bulk relaxation process sandwiched between blocking contacts[17]. The ionic conductivities (σ_i) of the LiSiON thin films can be calculated by using Eq. (1).

$$\sigma_i = d/(RA) \tag{1}$$

where d is the film thickness, A is the effective area (about 1 cm^2), and R is the film resistance estimated from the measured Nyquist plot. The calculated ionic conductivities for these LiSiON thin films are compared in Table 1. As observed, the ionic conductivity of the LiSiON thin film deposited at a constant flow of 90 sccm N$_2$ increases with the increasing sputtering power from 80 W to 100 W, then decreases when the sputtering power is further elevated to 120 W, which is similar to previous report on LiPON electrolyte[18]. An obvious increment in the ionic conductivities can be observed when the N$_2$ ratio in the working gas under a constant sputtering power of 100 W is promoted, which can be attributed to the increased amount of incorporated nitrogen in the LiSiON with more favorable environment for lithium ion motion[5, 18]. Noticeably, the sample LiSiON-100N9 and LiSiON-100N9A1 show the highest ionic conductivities of 7.1×10^{-6} and 6.3×10^{-6} S·cm^{-1}, respectively, which are obviously higher than the well-known LiPON (~2×10^{-6} S·cm^{-1}), previous reported amorphous LiNbO$_3$ (~1×10^{-6} S·cm^{-1})[19], LiBON (2.3×10^{-6} S·cm^{-1})[20], Li-V-Si-O (~1×10^{-6} S·cm^{-1})[21], Li-La-Zr-O (4×10^{-7} S·cm^{-1})[22], and Li-Si-P-O (1.6×10^{-6} S·cm^{-1})[23] electrolyte films, revealing that the amorphous LiSiON thin film is a competitive candidate as electrolyte for TFLB. The high ion conductivity of the LiSiON thin film can be attributed to the incorporation of N into the thin film and the formation of Si−N bonds instead of Si−O bonds,

leading to a more reticulated anionic network for the facile lithium ion mobility[17, 24]. The electrochemical stable voltage windows of the LiSiON thin films were evaluated by CV measurement at a scan rate of 5 mV·s^{-1} with voltage up to 5.5 V. It should be pointed out that the impact of deposition condition on the voltage window of LiSiON films varies, which cannot be explained by a clear mechanism currently since there are no relevant researches in previous reports about thin film electrolyte[18,24-25]. Nevertheless, as compared in Fig. 3(c) and Table 1, the sample LiSiON-100N9A1 and LiSiON-100N5A5 show the broadest voltage windows of ~5.0 and
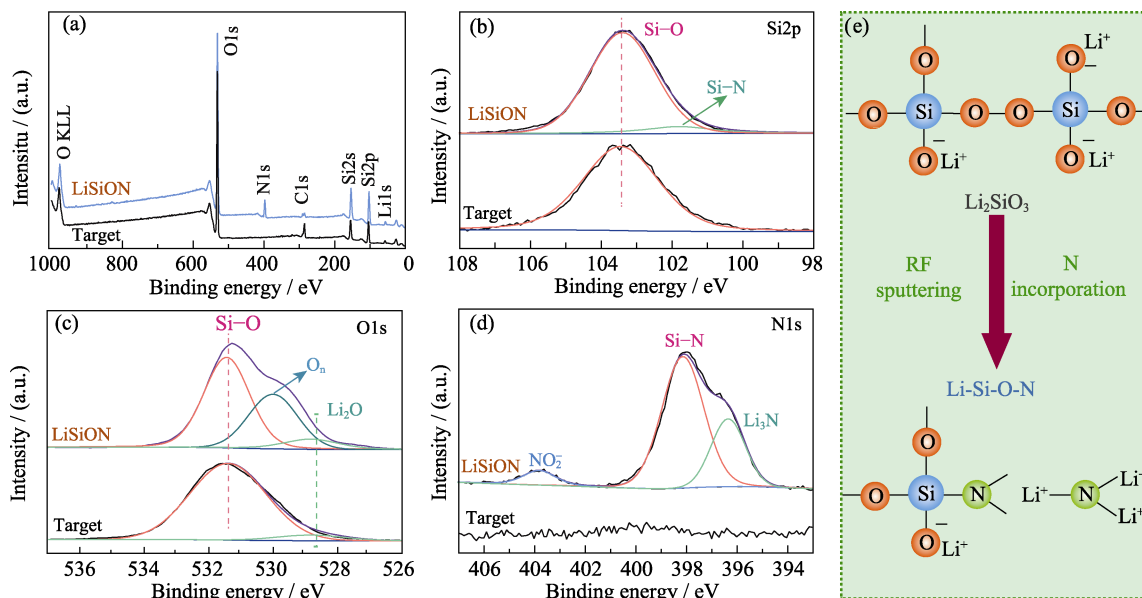

Fig. 2   (a) Survey-scan, (b) Si2p core-level, (c) O1s core-level, and (d) N1s core-level XPS spectra of Li$_2$SiO$_3$ target and typical sample LiSiON-100N9A1; (e) Schematic illustration of the partial structure change from Li$_2$SiO$_3$ to LiSiON with the incorporation of N
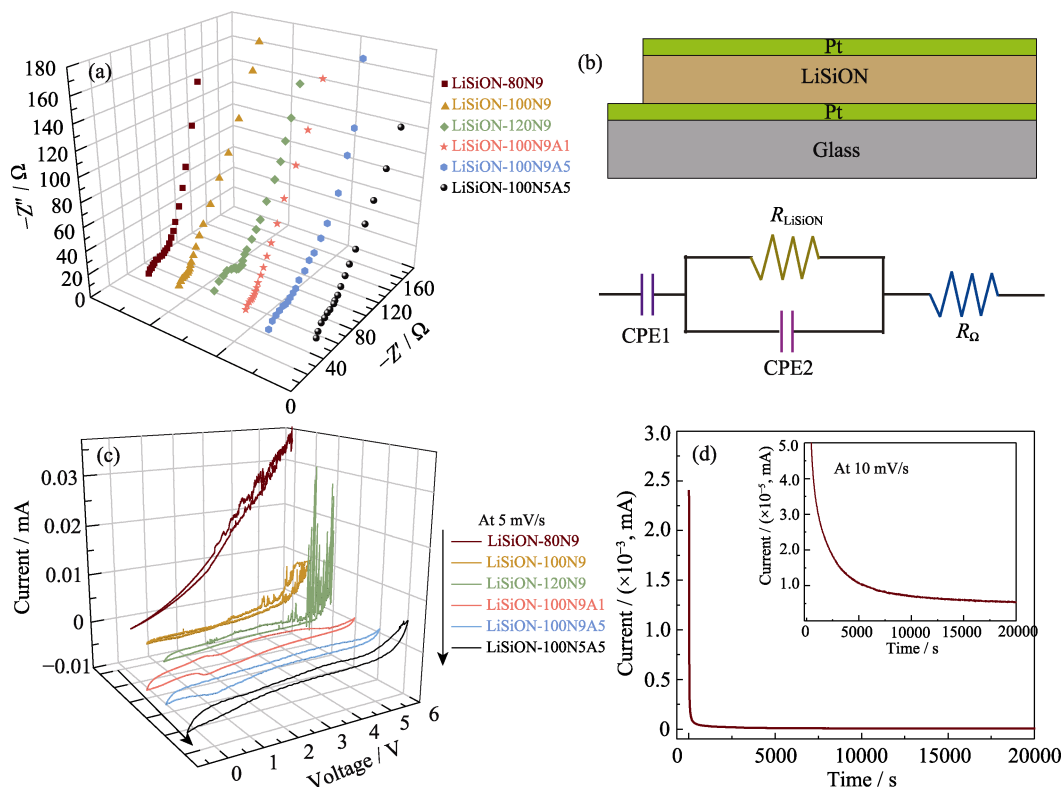

Fig. 3   (a) Electrochemical impedance spectroscopy (EIS) spectra of the LiSiON thin films deposited under different conditions; (b) Schematic illustration of the Pt/LiSiON/Pt sandwich structure and the corresponding equivalent circuit; (c) CV curves of the LiSiON thin films deposited under different conditions; (d) Chronoamperometry curve of the sample LiSiON-100N9A1

Table 1   Comparison of lithium ion conductivities and voltage windows of LiSiON thin films deposited under different conditions

Sample	Lithium ion conductivities /($\times 10^{-6}$, S·cm^{-1})	Voltage windows/V
LiSiON-80N9	4.6	~2.0
LiSiON-100N9	7.1	~3.9
LiSiON-120N9	2.5	~4.2
LiSiON-100N9A1	6.3	~5.0
LiSiON-100N9A5	3.0	~4.6
LiSiON-100N5A5	2.9	~5.2

~5.2 V, respectively, which are close to that of LiPON electrolyte. Therefore, taken both the ionic conductivity and voltage window into consideration, sample LiSiON-100N9A1 was chosen for further investigation and the fabrication of full cell. To explore the lithium ion transference number (τ_i) and the electronic conductivity (σ_e) of sample LiSiON-100N9A1, chronoamperometry was further performed at a constant voltage of 10 mV (Fig. 3(d)). The τ_i can be calculated by Eq. (2).

$$\tau_i = (I_b - I_e)/I_b \qquad (2)$$

where I_b is the initial polarization current, and I_e is the steady state current[18]. The τ_i was calculated to be 0.998, which is close to 1, indicating that the lithium ions conduction is absolutely dominant in the electrolyte. The τ_i is determined by a mixed effect of the conduction of ions and electrons[24], which can be expressed by Eq. (3).

$$\tau_i = \sigma_i/(\sigma_i + \sigma_e) \qquad (3)$$

Thus, the σ_e of the sample LiSiON-100N9A1 is calculated to be 1.26×10^{-8} S·cm^{-1}, which is negligible compared to its ion conductivity.

To verify the feasibility of the optimized sample LiSiON-100N9A1 for TFLB application, MoO$_3$/LiSiON/Li TFLB was further fabricated. The cross-section FESEM image and corresponding EDS mapping images of the MoO$_3$/LiSiON/Li TFLB are shown in Fig. 4(a). As observed, the MoO$_3$ cathode (about 1.1 μm in thickness) and the Li anode are well separated by the LiSiON
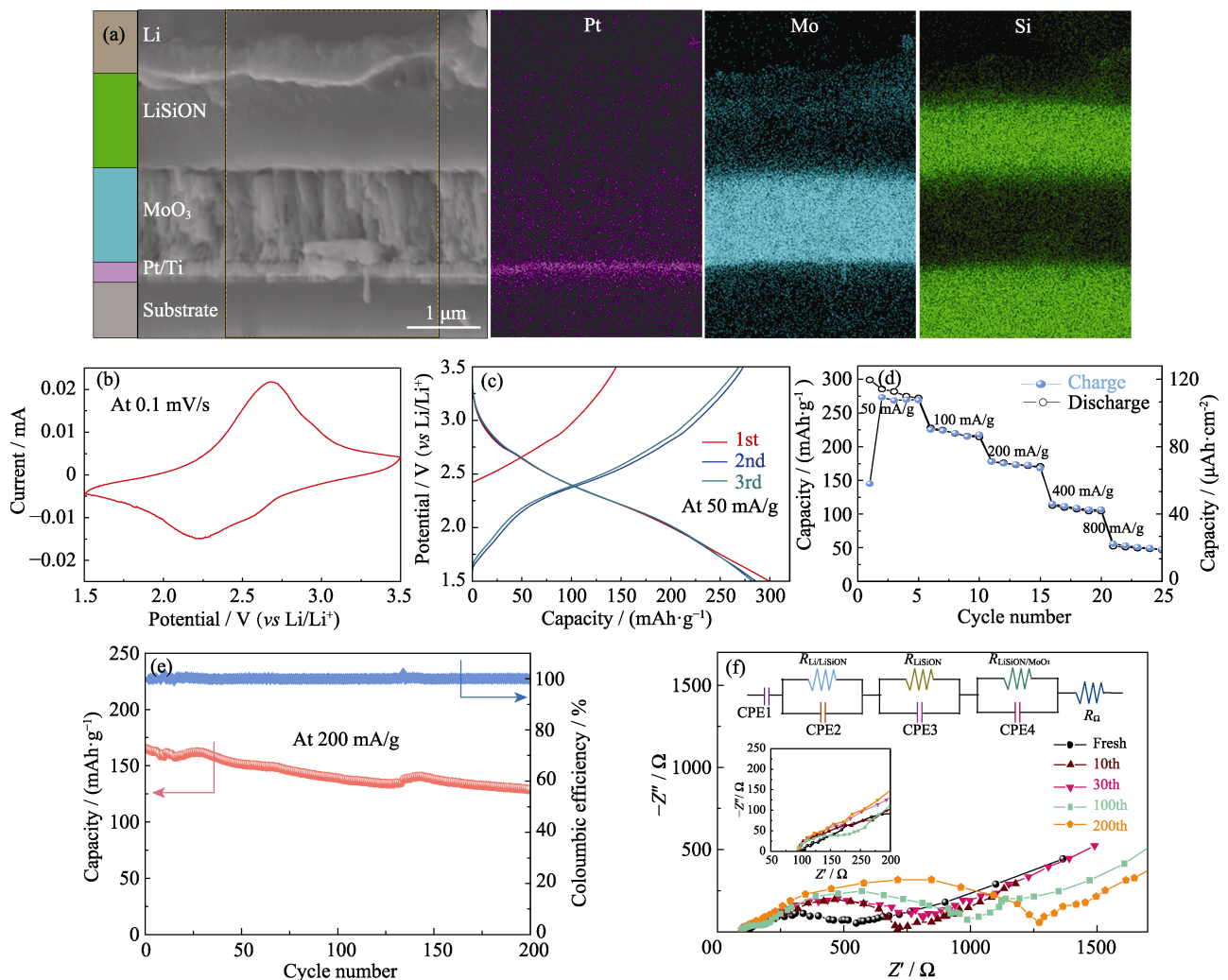

Fig. 4   (a) Cross-section FESEM image and corresponding EDS mapping images of the MoO$_3$/LiSiON/Li TFLB; (b) Typical CV curve, (c) initial three charge/discharge curves, (d) rate performance, (e) cycle performance, and (f) EIS spectra at different cycle numbers of the MoO$_3$/LiSiON/Li TFLB with sample LiSiON-100N9A1 as electrolyte

electrolyte, and the LiSiON electrolyte has tight contact interfaces with both the cathode and the anode. Fig. 4(b) displays the typical CV curve of the TFLB at a scan rate of 0.1 mV·s^{-1} between 1.5–3.5 V, which shows a pair of well-defined redox peaks at around 2.25 and 2.65 V, corresponding to lithium ion insertion into and extraction from the MoO$_3$[10]. Fig. 4(c) depicts the initial 3 galvanostatic charge/discharge curves of the TFLB at a current density of 50 mA·g^{-1} (20 μA·cm^{-2}, based on the mass of MoO$_3$ film). As observed, the TFLB delivers the initial charge/discharge capacities of 145/297 mAh·g^{-1} (58/118.8 μAh·cm^{-2}). After the 2nd cycle, steady cycling behavior with high reversible specific capacity of 282 mAh·g^{-1} was achieved by the TFLB. The rate performance of the TFLB at various current densities is depicted in Fig. 4(d). The irreversible capacity loss of the TFLB in initial several cycles at low current density can be attributed to irreversible phase transition in the MoO$_3$ derived by lithium insertion[26]. Stable discharge capacities of about 219, 173, 107, and 50 mAh·g^{-1} are observed at 100, 200, 400, and 800 mA·g^{-1}, respectively, demonstrating good rate capability. To evaluate the electrochemical stability of the TFLB, cycle performance was further performed at a current density of 200 mA·g^{-1} (Fig. 4(e)). The TFLB can retain 78.1% of its initial discharge capacity after 200 cycles, and the Coulombic efficiency is near 100% for each cycle, revealing acceptable electrochemical stability of the LiSiON electrolyte. EIS measurements were further carried out at open circuit voltage to investigate the electrolyte/electrode interface in the TFLB at different cycle numbers, and the corresponding Nyquist plots with equivalent circuit are depicted in Fig. 4(f). As observed, the MoO$_3$/LiSiON/Li TFLB shows similar EIS spectrum which consists of two semicircles in the high frequency region at fresh state to that of the MoO$_3$/LiPON/Li TFLB in our previous work[10], indicating that the Li/LiSiON interfacial resistance is negligible compared to that of the LiSiON/MoO$_3$ interface[20]. The first small semicircle in the Nyquist plots is attributed to the ionic conduction of Li$^+$ ions in LiSiON electrolyte, while the second large semicircle corresponds to the charge transfer process at the LiSiON/MoO$_3$ interface[27-28]. It is noted that the first small semicircle rarely changes during the cycles, indicating the relatively good cyclic stability of the LiSiON electrolyte. However, the second semicircle gradually expands as the cycle number evolves, revealing the increased LiSiON/MoO$_3$ interfacial resistance during cycling, which could be the main reason for the capacity fading of the TFLB[29]. It is worth mentioning that this work successfully adopts the LiSiON electrolyte to construct TFLB and demonstrates the good interfacial contact of LiSiON with both the MoO$_3$ cathode and the lithium anode for the first time. Moreover, the large specific capacity, good rate capability, and acceptable cycle performance of the MoO$_3$/LiSiON/Li TFLB demonstrate that the LiSiON thin film is well applicable as electrolyte for TFLB.

3   Conclusions

In summary, amorphous LiSiON thin film electrolyte was successfully prepared by RF magnetron sputtering using Li$_2$SiO$_3$ target with N$_2$/Ar gas flow. The optimized LiSiON thin film deposited under RF power of 100 W at the flow of 90 sccm N$_2$ and 10 sccm Ar possesses smooth surface, dense structure, high ion conductivity (6.3×10^{-6} S·cm^{-1}), and wide voltage window (5 V), making it a promising electrolyte material for TFLB. More importantly, by using the LiSiON electrolyte, a MoO$_3$/LiSiON/Li TFLB was successfully demonstrated for the first time with high specific capacity (282 mAh·g^{-1} at 50 mA·g^{-1}), good rate performance (50 mAh·g^{-1} at 800 mA·g^{-1}), and acceptable cycle stability (78.1% capacity retention after 200 cycles). This work is expected to bring new opportunities to develop high- performance TFLB by using Li$_2$O-SiO$_2$ based thin film electrolyte.

References:

[1] MOITZHEIM S, PUT B, VEREECKEN P M. Advances in 3D thin-film Li-ion batteries. *Advanced Materials Interfaces*, 2019, **6(15):** 1900805.

[2] XIA Q, ZHANG Q, SUN S, et al. Tunnel intergrowth Li$_x$MnO$_2$ nanosheet arrays as 3D cathode for high-performance all-solid-state thin film lithium microbatteries. *Advanced Materials*, 2021, **33(5):** 2003524.

[3] DENG Y, EAMES C, FLEUTOT B, et al. Enhancing the lithium ion conductivity in lithium superionic conductor (LISICON) solid electrolytes through a mixed polyanion effect. *ACS Applied Materials & Interfaces*, 2017, **9(8):** 7050–7058.

[4] BATES J B, DUDNEY N J, GRUZALSKI G R, et al. Fabrication and characterization of amorphous lithium electrolyte thin films and rechargeable thin-film batteries. *Journal of Power Sources*, 1993, **43(1/2/3):** 103–110.

[5] BATES J. Electrical properties of amorphous lithium electrolyte thin films. *Solid State Ionics*, 1992, **53(56):** 647–654.

[6] FAMPRIKIS T, GALIPAUD J, CLEMENS O, et al. Composition dependence of ionic conductivity in LiSiPO(N) thin-film electrolytes for solid-state batteries. *ACS Applied Energy Materials*, 2019, **2(7):** 4782–4791.

[7] DENG Y, EAMES C, CHOTARD J N, et al. Structural and mechanistic insights into fast lithium-ion conduction in Li$_4$SiO$_4$-Li$_3$PO$_4$ solid electrolytes. *Journal of the American Chemical Society*, 2015, **137(28):** 9136–9145.

[8] CHEN R, SONG X. The ionic conductivity of solid electrolytes for Li$_{4+x}$M$_x$Si$_{1-x}$O$_4$-$_y$Li$_2$O (M=Al, B) systems. *Journal of the Chinese Chemical Society*, 2002, **49:** 7–10.

[9] ADNAN S, MOHAMED N S. Effects of Sn substitution on the properties of Li₄SiO₄ ceramic electrolyte. *Solid State Ionics*, 2014, **262:** 559–562.

[10] SUN S, XIA Q, LIU J, *et al*. Self-standing oxygen-deficient *α*-MoO₃₋ₓ nanoflake arrays as 3D cathode for advanced all-solid-state thin film lithium batteries. *Journal of Materiomics*, 2019, **5(2):** 229–236.

[11] DING W, LU W, DENG X, *et al*. An XPS study on the structure of SiNₓ film deposited by microwave ECR magnetron sputtering. *Acta Physica Sinica*, 2009, **58(6):** 4109–4116.

[12] KIM H, KIM Y. Partial nitridation of Li₄SiO₄ and ionic conductivity of Li₄.₁SiO₃.₉N₀.₁. *Ceramics International*, 2018, **44(8):** 9058–9062.

[13] MARIKO M, HIDEMASA K ,TOMOYUKI O, *et al*. Analysis of SiO anodes for lithium-ion batteries. *Journal of The Electro-chemical Society*, 2005, **152(10):** A2089.

[14] FINGERLE M, BUCHHEIT R, SICOLO S, *et al*. Reaction and space charge layer formation at the LiCoO₂-LiPON interface: insights on defect formation and ion energy level alignment by a combined surface science–simulation approach. *Chemisty Materials*, 2017, **29(18):** 7675–7685.

[15] WEST W, HOOD Z, ADHIKARI S, *et al*. Reduction of charge-transfer resistance at the solid electrolyte-electrode interface by pulsed laser deposition of films from a crystalline Li₂PO₂N source. *Journal of Power Sources*, 2016, **312:** 116–122.

[16] SICOLO S, FINGERLE M, HAUSBRAND R, *et al*. Interfacial instability of amorphous LiPON against lithium: a combined density functional theory and spectroscopic study. *Journal of Power Sources*, 2017, **354:** 124–133.

[17] WU F, LIU Y, CHEN R, *et al*. Preparation and performance of novel Li-Ti-Si-P-O-N thin-film electrolyte for thin-film lithium batteries. *Journal of Power Sources*, 2009, **189(1):** 467–470.

[18] PUT B, VEREECKEN M, MEERSSCHAUT J, *et al*. Electrical characterization of ultrathin RF-sputtered LiPON layers for nanoscale batteries. *ACS Applied Materials & Interfaces*, 2016, **8(11):** 7060−7069.

[19] NIINOMI H, MOTOYAMA M, IRIYAMA Y. Li⁺ Conduction in Li-Nb-O films deposited by a Sol–Gel method. *Solid State Ionics*, 2016, **285:** 13–18.

[20] SONG S, LEE K, PARK H. High-performance flexible all-solid-state microbatteries based on solid electrolyte of lithium boron oxynitride. *Journal of Power Sources*, 2016, **328:** 311–317.

[21] OHTSUKA H, OKADA S, YAMAKI J. Solid state battery with Li₂O-V₂O₅-SiO₂ solid electrolyte thin film. *Solid State Ionics*, 1990, **40–41:** 964–966.

[22] Kalita D, Lee S, Lee K, *et al*. Ionic conductivity properties of amorphous Li-La-Zr-O solid electrolyte for thin film batteries. *Solid State Ionics*, 2012, **229:** 14–19.

[23] SAKURAI Y, SAKUDA A, HAYASHI A, *et al*. Preparation of amorphous Li₄SiO₄-Li₃PO₄ thin films by pulsed laser deposition for all-solid-state lithium secondary batteries. *Solid State Ionics*, 2011, **182:** 59–63.

[24] TAN G, WU F, LI L, *et al*. Magnetron sputtering preparation of nitrogen-incorporated lithium-aluminum-titanium phosphate based thin film electrolytes for all-solid-state lithium ion batteries. *The Journal of Physical Chemistry C*, 2012, **116(5):** 3817–3826.

[25] YU X, BATES J B, JELLISON G, *et al*. A stable thin-film lithium electrolyte: lithium phosphorus oxynitride. *Journal of The Electro-chemical Society*, 1997, **144(2):** 524.

[26] KIM H, COOK J, LIN H, *et al*. Oxygen vacancies enhance pseudocapacitive charge storage properties of MoO₃₋ₓ. *Nature Materials*, 2017, **16:** 454–460.

[27] SONG H, WANG S, SONG X, *et al*. Solar-driven all-solid-state lithium-air batteries operating at extreme low temperatures. *Energy & Environmental Science*, 2020, **13(4):** 1205–1211.

[28] WANG Z, LEE J, XIN H, *et al*. Effects of cathode electrolyte interfacial (CEI) layer on long term cycling of all-solid-state thin-film batteries. *Journal of Power Sources*, 2016, **324:** 342–348.

[29] QIAO Y, DENG H, HE P, *et al*. A 500 Wh/kg lithium-metal cell based on anionic redox. *Joule*, 2020, **4(6):** 1311–1323.

非晶 LiSiON 薄膜电解质的全固态薄膜锂电池性能

夏求应, 孙 硕, 昝 峰, 徐 璟, 夏 晖

(南京理工大学 材料科学与工程学院, 南京 210094)

摘 要: 全固态薄膜锂电池(TFLB)是理想的微电子系统电源。目前报道的固态非晶电解质存在离子电导率偏低的问题, 限制了 TFLB 性能的提升。本工作采用磁控溅射法制备了一种新型非晶锂硅氧氮(LiSiON)薄膜用作 TFLB 的固态电解质。结果表明, 优化制备条件后的 LiSiON 薄膜具有 6.3×10^{-6} S·cm⁻¹ 的高离子电导率以及超过 5 V 的宽电压窗口, 适合作为 TFLB 的电解质。在 LiSiON 薄膜电解质的基础上, 本工作构建了 MoO₃/LiSiON/Li TFLB 并获得高的比容量(50 mA·g⁻¹ 下 282 mAh·g⁻¹)、良好的倍率性能(800 mA·g⁻¹ 下 50 mAh·g⁻¹)和可观的循环寿命(200 次循环后容量保持率为 78.1%), 验证了该电解质在薄膜电池中应用的可行性。

关 键 词: LiSiON; 薄膜电解质; 全固态锂电池; 薄膜电池

中图分类号: TQ174 **文献标志码:** A